2-5-1989

The Three-dimensional Structure of Bovine Platelet Factor 4 at 3.0-Å Resolution

Robert St. Charles
Wayne State University School of Medicine

Daniel A. Walz
Wayne State University School of Medicine

Brian FP Edwards
Department of Biochemistry, Wayne State University School of Medicine, bedwards@med.wayne.edu

Recommended Citation

St. Charles, R., Walz, D. A., and Edwards, B. F. P. The three-dimensional structure of bovine platelet factor 4 at 3.0 Å resolution. J. Biol. Chemistry 264: 2092-2099, 1989. https://doi.org/10.1016/s0021-9258(18)94146-3

THE JOURNAL OF BIOLOGICAL CHEMISTRY

Vol. 264, No. 4, Issue of February 5, pp. 2092-2099, 1989
Printed in U.S.A.

The Three-dimensional Structure of Bovine Platelet Factor 4 at 3.0-Å Resolution*

(Received for publication, September 9, 1988)

Robert St. Charles‡, Daniel A. Walz, and Brian F. P. Edwards§

From the Departments of Biochemistry and Physiology, Wayne State University School of Medicine, Detroit, Michigan 48201

Platelet factor 4 (PF4), which is released by platelets during coagulation, binds very tightly to negatively charged oligosaccharides such as heparin. To date, six other proteins are known that are homologous in sequence with PF4 but have quite different functions. The structure of a tetramer of bovine PF4 complexed with one $Ni(CN)_4^{2-}$ molecule has been determined at 3.0 Å resolution and refined to an *R* factor of 0.28. The current model contains residues 24–85, no solvent, and one overall temperature factor. Residues 1–13, which carried an oligosaccharide chain, were removed with elastase to induce crystallization; residues 14–23 and presumably 86–88 are disordered in the electron density map. Because no heavy atom derivative was isomorphous with the native crystals, the complex of PF4 with one $Ni(CN)_4^{2-}$ molecule was solved using a single, highly isomorphous $Pt(CN)_4^{2-}$ derivative and the iterative, single isomorphous replacement method.

The secondary structure of the PF4 subunit, from amino- to carboxyl-terminal end, consists of an extended loop, three strands of antiparallel β-sheet arranged in a Greek key, and one α-helix. The tetramer contains two extended, six-stranded β-sheets, each formed by two subunits, which are arranged back-to-back to form a "β-bilayer" structure with two buried salt bridges sandwiched in the middle. The carboxyl-terminal α-helices, which contain lysine residues that are thought to be intimately involved in binding heparin, are arranged as antiparallel pairs on the surface of each extended β-sheet.

Platelet factor 4 (PF4)[1] is carried within the α-granules of platelets in the form on a noncovalent complex with a proteoglycan carrier (Barber *et al.*, 1972). PF4 is a tetramer (Bock *et al.*, 1980) of four identical polypeptide chains, each of which contains 88 residues (M_r = 9580) in the bovine molecule (Ciaglowski *et al.*, 1986) or 70 residues in the human (Deuel *et al.*, 1977; Hermodson *et al.*, 1977; Morgan *et al.*, 1977; Walz *et al.*, 1977). The human and bovine sequences are 73% identical.

When released into the plasma from activated platelets, PF4 attracts white blood cells, *i.e.* neutrophils and monocytes, and its release may be the signal that initiates inflammation (Deuel *et al.*, 1981). Other possible functions of PF4 derive from its strong binding to negatively charged polysaccharides, especially heparan and heparin, for which it has a dissociation constant of $10^{-7.5}$ (Loscalzo *et al.*, 1985). The ability of PF4 to neutralize heparin and related polymers is of general interest because heparin has been shown to interact with over 50 enzymes (Machovich, 1984), to suppress smooth muscle growth (Castellot *et al.*, 1982), and to accelerate angiogenesis in solid tumors (Taylor and Folkman, 1982). PF4 has recently been patented as "Oncostatin A" for its ability to inhibit tumor growth (Twardzik and Todaro, 1987). It also has been shown to reverse immunosuppression in mice (Katz *et al.*, 1986).

Platelet factor 4 also binds tightly and preferentially to double-stranded DNA *in vitro*.[2] This binding probably does not occur *in vivo*, but it might be an important attribute of several recently discovered, growth-related proteins that are homologous to PF4. Members of this class are 1) induced by γ-interferon (Luster *et al.*, 1985), 2) constitutively overexpressed in transformed Chinese hamster and human cell lines (Anisowicz *et al.*, 1987), 3) strongly induced by Rous sarcoma virus in fibroblast cell lines (Sugano *et al.*, 1987; Bedard *et al.*, 1987), and 4) overexpressed in stimulated leukocytes (Schmid and Weissmann, 1987; Walz *et al.*, 1987; Yoshimura *et al.*, 1987).

Another homolog of PF4 that has been known for some time in the human platelet system is β-thromboglobulin and its two precursors, platelet basic protein (Holt *et al.*, 1986) and low affinity platelet factor 4 (Rucinski *et al.*, 1979), which is also named connective tissue activating protein III (Castor *et al.*, 1983). Collectively, these proteins appear to be involved in inflammation and wound healing (Senior *et al.*, 1983).

When released by activated platelets during coagulation, PF4 displaces thrombin from the heparan on the surface of endothelial cells, where thrombin is anticoagulant through its accelerated interactions with antithrombin III (AT-III), thrombomodulin, and protein C, into solution, where thrombin is procoagulant through its interactions with fibrinogen and other clotting factors (Stern *et al.*, 1985; Loscalzo *et al.*, 1985). It also prevents the formation of the ternary complexes between heparin, AT-III, and various procoagulant serine proteases that are intermediate in the heparin-accelerated inhibition of proteases by AT-III (Rosenberg and Damus, 1973; Laurent *et al.*, 1978).

The strongest binding between heparin and PF4 requires heparin molecules above 10,000 daltons in size or approxi-

* This work was supported by National Institutes of Health Grants GM 33912, HL 27073, and RR 02945, and grants-in-aid from the American Heart Association of Michigan, and the Wayne State University Center for Molecular Biology. The costs of publication of this article were defrayed in part by the payment of page charges. This article must therefore be hereby marked "*advertisement*" in accordance with 18 U.S.C. Section 1734 solely to indicate this fact.

‡ Recipient of a predoctoral Traineeship T32 HL 07602 from National Heart, Lung and Blood Institute.

§ To whom reprint requests should be addressed: Dept. of Biochemistry, Wayne State University, 540 E. Canfield Ave., Detroit, MI 48201.

[1] The abbreviations used are: PF4, platelet factor 4; AT-III, antithrombin III; HLA-A2, human class I histocompatibility antigen form A2; ISIR, iterative single isomorphous replacement; β-TG, β-thromboglobulin.

[2] P. Johnson, personal communication.

mately 16 saccharide units (Luscombe and Holbrook, 1983; Denton *et al.*, 1983). Luscombe and Holbrook (1983) postulated that the critical size arises from the heparin winding around the outside of a globular protein core. From small angle neutron scattering experiments (Ibel *et al.*, 1986), they were able to calculate a radius of 2.11 nm for the PF4 core and an average radius of 2.5 nm for the heparin coiled around the core.

A similar model has also been developed from x-ray diffraction data by Cowan *et al.* (1986). They used the packing density of human PF4 crystals (Kurachi, 1978; Machin and Isaacs, 1984) and a rotation function confirming 222 symmetry in the PF4 tetramer to deduce a model in which the PF4 core, represented as four tetrahedrally arranged spheres of radius 1.6 nm, had an overall radius of 3.6 nm. Using this method, they proposed that a 16-saccharide heparin coil with a radius of 1.7 nm could reach all four heparin binding sites on the PF4 tetramer. Although these models are undoubtedly correct in their overall concepts, they are based on very limited structural information. In this paper we present a refined model of bovine PF4 at 3.0 Å resolution.

MATERIALS AND METHODS

Preparation of PF4 Crystals—Platelet factor 4 was purified from bovine platelets as described by Ciaglowski *et al.* (1981); it was crystallized in space group $P2_12_12_1$ with $a = 63.7$ Å, $b = 66.7$ Å, $c = 80.5$ Å, and a tetramer of 32,000 daltons in the asymmetric unit, as described by St. Charles *et al.* (1984) with the modification that the protein was treated with porcine elastase prior to crystallization. After the initial report was published, we discovered that the first 13 amino acids, which included an oligosaccharide, must be removed from the amino-terminal end of bovine PF4 before it will crystallize. An endogenous, contaminating protease removed these residues in our original crystallizations; however, we have found that porcine elastase will also catalyze the conversion with the advantage that it is faster and more controllable.

On this basis, PF4 could be reproducibly crystallized as follows. A 10–20 mg/ml solution of PF4 in 50 mM Tris, pH 8.0, was prepared and treated with porcine elastase (1:1000, w/w) for 0.5 h at 25 °C. The insoluble suspension was spun at 1200 × *g* for 30 s and the resulting oily pellet washed with several volumes of cold, 50 mM Tris buffer, pH 8.0. The pellet was dissolved in enough 0.4 M NaCl, 50 mM Tris-HCl, pH 8.0, to give a final protein concentration of 10 mg/ml. This solution was set up in a hanging drop or nested dish arrangement (5–20 μl) and allowed to vapor-equilibrate against 0.02–0.14 M NaCl. Crystals 0.5 × 0.5 × 1.0 mm in size were obtained within 1–2 weeks. They were stored in a stabilizing buffer of 20 mM Tris, pH 8.0.

Data Collection—Diffraction data were collected to 3.0 Å resolution on two crystals for both the nickel and platinum derivatives (Table I). The intensities were measured on a Nicolet/Syntex $P2_1$ four circle diffractometer, which had been modified for protein data collection with an extended detector arm and a 385-mm-long, helium-filled beam tunnel. The ω scan of the reflection, which was taken over 0.33° at 0.66°/min, was broken into 11 steps, of which the best seven were kept for the intensity measurement. The nickel-filtered, copper K_α x-rays were generated at 40 kV, 25 mA. Crystals were mounted in glass capillaries with the long axis of the crystal, which was parallel to the crystallographic *a*-axis, aligned along the spindle axis.

TABLE I
Diffraction data

Crystal[a]	Limits	Total[b]	Used[c]	R_{sym}[d]	Decay	R_{mrg}[e]
	Å					
Nickel 1	10–3.6	4103	4028	0.051	0.15	
Nickel 2	3.8–3.0	3653	3454	0.039	0.16	
Nickel merged	10–3.0	7096	6912			0.044
Platinum 1	10–3.6	4098	3986	0.040	0.28	
Platinum 2	3.8–3.0	3671	3474	0.036	0.18	
Platinum merged	10–3.0	7080	6901			0.047

[a] "Nickel" is elastase-treated bovine PF4 reacted with $K_2Ni(CN)_4$; "platinum" is elastase-treated bovine PF4 reacted with $K_2Pt(CN)_4$.

[b] Total relections possible within the resolution limits.

[c] Number of reflections with an intensity greater than twice the standard deviation.

[d] $R_{sym} = \sum | \; | F_i | - | F_k | \; | / \sum | F_i |$ summed over all symmetry equivalent pairs of reflections *i* and *k*.

[e] $R_{mrg} = \sum | I_i - \langle I \rangle_k | / \sum | \langle I \rangle_i |$ summed over all *i* data sets for all *k* reflections used. $\langle I \rangle_k$ is the average intensity for reflection *k*.

The intensity data were processed using the PROTSYS package of crystallographic programs implemented on a VAX 11/780 computer. Individual backgrounds were not collected. Instead, an empirical correction was calculated as a function of 2θ and ϕ (Krieger *et al.*, 1974). This approach saves significant time in the data collection and gives R_{sym} values for protein data that are equal or better than those from the traditional method. Radiation damage was corrected from a linear least squares analysis of four monitor reflections. The absorption correction was calculated by the method of North *et al.* (1968) from measurements on two strong axial reflections (*h*00) collected over a 180° range in ϕ in 15° increments.

For each derivative, the data were collected from 10 to 3.6 and 3.8 to 3.0 Å on two crystals. Scaling and merging of the partial data sets was done with the DIFCOR program in the ROCKS suite of crystallographic programs (Reeke, 1984) using the overlapping 3.6–3.8 Å data together with 10–2.9 Å 0*kl* data which were also collected on each crystal.

Determination of the Phases—An exhaustive search for heavy atom derivatives, over a period of 2 years, failed to identify any heavy atom reagents that would produce site-specific derivatives isomorphous with the native crystals. Crystals of PF4 were found to be quite fragile and susceptible to cracking upon exposure to submillimolar concentrations of heavy atom salts. However, potassium platinum tetracyanide ($K_2Pt(CN)_4 \cdot 3H_2O$) generated an excellent, albeit nonisomorphous derivative, as evidenced by a regular fracture pattern in the crystals, by precession photographs showing a larger unit cell, and by the retention of the high angle intensities. The unit cell axes *a*, *b*, and *c* were, respectively, 0.16, 1.45, and 0.25 Å longer than those of the native crystals. These observations offered the possibility that a light atom analog could be used to prepare parent crystals isomorphous with the platinum derivative. An isomorphous parent "derivative" was prepared by treating native crystals with the chemically analogous complex, potassium nickel tetracyanide ($K_2Ni(CN)_4$). In both cases, derivatization was accomplished by slow diffusion of the complex over a 2-day period. The crystals were placed in 200 μl of stabilizing buffer in a microdialysis cell and floated on top of 5 ml of stabilizing buffer containing 0.2 mM reagent. The dialysis cell was prepared from a 1.5-ml Eppendorf centrifuge tube. The center was removed from the cap, the tube below the upper rim was cut off, and dialysis membrane was then clamped between the cap and the rim.

Patterson maps based on the differences in diffraction intensities and anomalous scattering between platinum and nickel derivatives indicated a single site of substitution. It was used to calculate initial phases for the nickel derivative as the "native" from the equations for single isomorphous replacement. These phases were then refined by the iterative method of Wang (1985).

Electron Density Fitting—The main chain of the four monomers in the crystallographic asymmetric unit were fit independently. Then the noncrystallographic symmetry transformation between the monomer with the best overall electron density (monomer A) and the other three subunits were calculated by least squares methods from the positions of equivalent mainchain C_α atoms. Side chains for monomer A were then fit into the density. Since the monomers appeared to be very similar, we rotated and translated the completed A-monomer into the density for the other three monomers. No major adjustments in the side chains of the other monomers were necessary before refinement started. During refinement we examined regions that had a questionable fit with $2F_o - F_c$ electron density maps. As a final check of the model, we stepped through the entire sequence of the tetramer in 24 consecutive "fragment-deleted" maps. The segment in question, usually 11 residues, was removed from the model, five cycles of restrained least squares (Hendrickson and Konnert, 1980) were run, and then a $2F_o - F_c$ electron density map was calculated.

Refinement—The model was refined by restrained least squares (Hendrickson and Konnert, 1980) in two stages. In the first stage the restraints were chosen to make the four subunits equivalent, residues 75–85 an ideal helix, and the torsion angle χ_3 of the cystines equal to ± 90°. The weighting factors were those recommended by Hendrickson (1985). In the second stage the subunits were independent, residues 75–85 were partially constrained to be helical, and the

cystines were as in stage 1. Due to the modest resolution of the diffraction data, individual temperature factors and solvent were not included.

RESULTS

The mean fractional isomorphous difference was 13.2% between the nickel and platinum data sets. Fig. 1 shows the Harker sections from the isomorphous difference Patterson map calculated using $|F_{Pt} - F_{Ni}|$ as coefficients in the synthesis. The single, well defined peak indicated one major binding site with fractional coordinates 0.064, 0.024, and 0.229, respectively, for x, y, and z. Early electron density maps phased with this solution were left-handed so the coordinates were inverted for subsequent calculations. This site was also observed in an anomalous difference Patterson synthesis using anomalous difference data measured on the $K_2Pt(CN)_4$ derivative (data not shown). The occupancy and positional parameters of the single heavy atom site were refined by full-matrix least squares. The final R factor, using 10–3.0 Å data and simple difference data, was 0.54 after 12 cycles of refinement.

The mean figure of merit of the initial, single isomorphous replacement phase set was 0.34. The phases were refined by the iterative single isomorphous replacement (ISIR) method (Wang, 1985). A solvent mask was prepared from the starting SIR phases using all data to 3.0 Å. This mask was then used for electron density filtering and phase refinement for four cycles. A second mask was calculated based on the refined

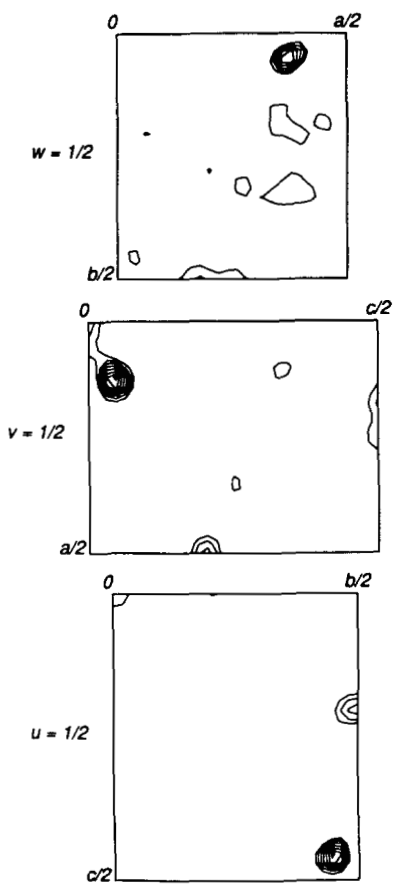

FIG. 1. **Patterson maps calculated from the intensity differences between the nickel and platinum data sets.** The three Harker sections for space group $P2_12_12_1$ (*a*) $U = 0.5$, (*b*) $V = 0.5$, and (*c*) $W = 0.5$ are shown with the first contour line representing 20% of the origin peak and each succeeding contour line representing an increment of 10%. Data between 10 and 4.2 Å were used in the calculation.

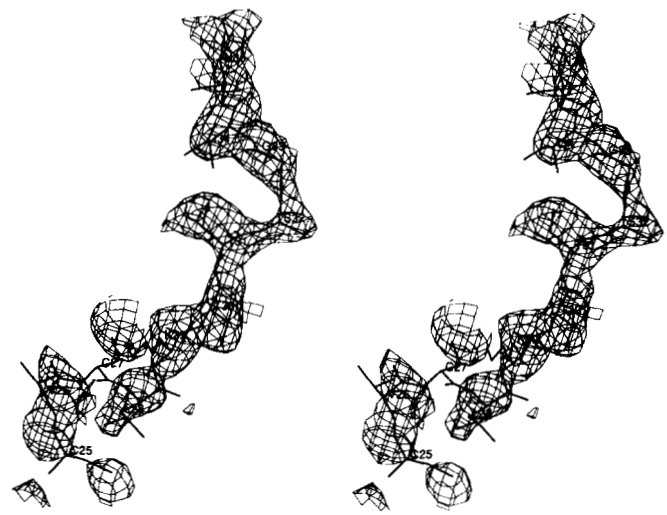

FIG. 2. **ISIR electron density map of the amino terminus.** The starting model for refinement of residues Cys-25 to Asn-35 is superimposed on the electron density map that was calculated at 3.0 Å resolution from the nickel derivative data and the ISIR phases.

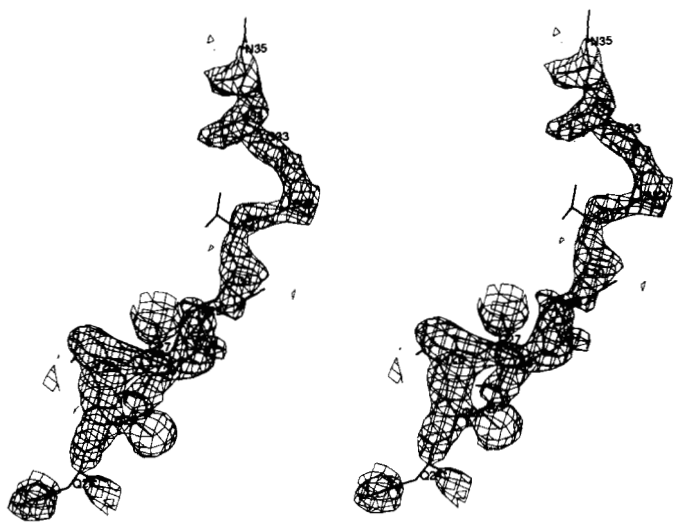

FIG. 3. **Final fragment-deleted electron density map of the amino terminus.** Residues Gln-24 to Asn-35 from the refined model of PF4 ($R = 0.28$) are superimposed on a $2F_o - F_c$ electron density map. The map was calculated after five cycles of restrained least squares refinement that did not include Gln-24 to Ile-34.

phases and the original SIR phases were refined using the second mask. After calculating a third solvent mask from these phases, the original phases were subjected to eight cycles of phase refinement resulting in a final mean figure of merit of 0.78. In effect, the 32,000-dalton PF4 structure was phased using a single, 50-electron heavy atom derivative.

In the original ISIR-phased map, we fit residues 25–85 of all four subunits by first fitting the well defined, main chain electron density in all four subunits. Transformation matrices among the subunits were calculated by least squares superposition of these individually fit pieces of main chain. We then fit the side chains and entire main chain in the A-subunit. Stretches of weaker electron density in the A-subunit, which were primarily in the amino-terminal region, were fit by comparison with equivalent but better defined regions in one or more of the other subunits. Fig. 2 shows our initial model for the amino terminus region of subunit A superimposed on the ISIR electron density. The amino-terminal

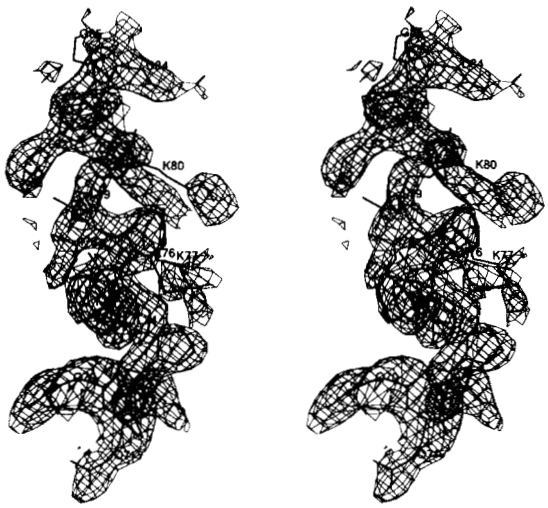

FIG. 4. **Final fragment-deleted electron density map of the carboxyl terminus.** Residues Gln-70 to Gly-85 from the refined model of PF4 (R = 0.28) are superimposed on a $2F_o - F_c$ electron density map. The map was calculated after five cycles of restrained least squares refinement that did not include the residues Tyr-75 to Gly-85.

section had the weakest density in all four subunits. The complete A-subunit was then rotated into the electron density of the other three subunits using the transformation matices.

After several false starts using the restrained least squares refinement program, we reduced the R factor from 0.49 to 0.28 in 50 cycles with an error of 0.019 Å in the bond lengths. In the early stages of the refinement we were able to locate Gln-24 in a $2F_o - F_c$ electron density map. Fig. 3 shows the final model for the amino-terminal region displayed in Fig. 2. Fig. 4 shows the final model for the carboxyl-terminal region of subunit A. Fig. 5 shows the entire C_α-backbone of the AB dimer after refinement. Different views of the C_α-backbone for all four subunits plus the side chains of selected residues are shown in Figs. 6 and 7. The final electron density map contained density for 62 of the 75 residues present in the elastase-treated PF4 (Asp-14 through Ser-88). No convincing electron density was seen for 10 residues on the amino-terminal end (Asp-14 through Gln-23) nor for the last 3 residues on the carboxyl-terminal end. By contrast, the disulfide bonds Cys-25 to Cys-51 and Cys-27 to Cys-67 were especially clear in the map.

DISCUSSION

For convenience in this discussion, we labeled as "A" the subunit that we fit in its entirety by manual methods, its partner in the extended β-sheet as "B," its nearest neighbor in the opposite β-sheet as "C," and its farthest neighbor "D." Residues 24–85 refer to monomer-A, which is used as the representative subunit of the PF4 tetramer because it interacts least with the nickel ion. Residues 124–185, 224–285, and 324–385 belong to subunits B, C, and D, respectively. Also, we have divided the tetramer into two nominal dimers consisting of the AB and CD monomers based on the presumed strength of the interactions among the subunits. There is no evidence for dimers existing independently in solution.

The major elements of secondary structure in the PF4 subunit, which are shown in stereo in Fig. 5 and diagrammatically in Fig. 8, are a 12-residue loop, three strands of antiparallel β-sheet, and a 12-residue helix. The helix, which is on the "outside" of the molecule, crosses the pleated sheet at an angle of approximately 52°. These elements place PF4 among the $\alpha + \beta$ class of protein structures (Creighton, 1984). The four subunits in the crystallographic asymmetric unit are paired to form two extended β-pleated sheets of six strands each (Fig. 5) which are then arranged back-to-back (Fig. 6) to form a tetramer. At physiological ionic strengths, human PF4 exhibits the molecular weight characteristic of a tetramer (Kaser-Glanzmann *et al.*, 1972; Bock *et al.*, 1980).

The PF4 tetramer in this crystal structure has approximate dimensions of 35 × 35 × 45 Å and a radius of gryation of 18.4 Å. Ibel *et al.* (1986) derived a value of 17.4 Å from neutron scattering experiments. The difference is probably due to a small expansion in the PF4 structure caused by the nickel ion. The symmetry of the four subunits is approximately 222, as expected, but it is distorted by the binding of the nickel ion between tetramers. The tetramer is far from being pseudo-tetrahedral as shown by the fact that the putative heparin binding sites are clearly grouped in pairs; the helices in the same dimer are separated by approximately 14 Å while those in different dimers are separated by approximately 36 Å. The tetramer is packed along the b-axis in the crystal with the basic carboxyl-terminal helices of its subunits next to the acidic amino-terminal ends of subunits in adjacent tetramers.

The structure of PF4 is unusual. The most similar structure is that of the α_1 and α_2 domains of the class I histocompatibility antigen, HLA-A2 (Bjorkman *et al.*, 1987). However, HLA-A2 differs from PF4 dimer in having an eight-stranded β-sheet, longer helices, and a greater separation between the helices. The widest separation between C_α atoms of the two helices in HLA-A2 (1HLA in the Brookhaven Protein Data Bank) is approximately 14 Å, which is wide enough to bind a peptide. The separation is approximately 10 Å in PF4. In addition, the helices in HLA-A2 cross the β-sheet at an angle of approximately −45° instead of the +52° found in PF4 dimers. Despite these differences the related motifs of the two proteins are provocative given that PF4 stimulates the immune system (Katz *et al.*, 1986). Sheet structures that extend across subunits also occur in dimers of prealbumin (Blake *et al.*, 1974), concanavalin A (Reeke *et al.*, 1975), alcohol dehy-

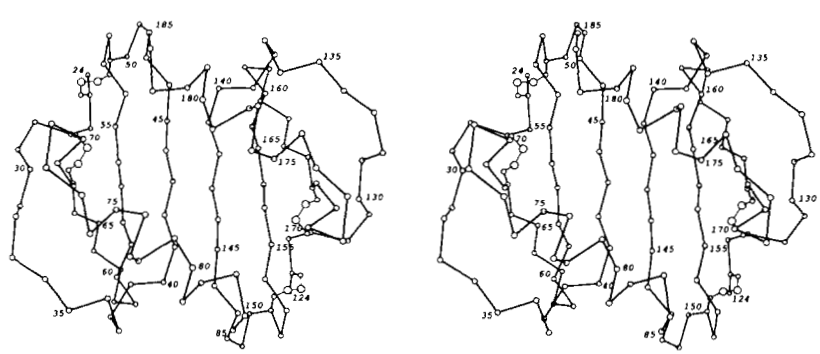

FIG. 5. **The PF4 dimer.** The α-carbon backbone of residues 24–85 (subunit A) and residues 124–185 (subunit B) from the refined model of PF4 are shown in stereo. The view is approximately down the AB noncrystallographic 2-fold axis. The positions of the C_α atoms are marked with small circles. The two cystine bonds near the amino-terminal end of each subunit are drawn with thin lines between the side chain atoms and large circles for the sulfur atoms.

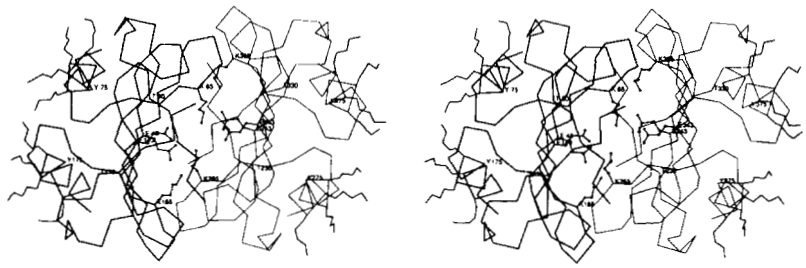

FIG. 6. **The PF4 tetramer with selected side chains.** The α-carbon backbone from the refined model of the PF4 tetramer is shown in stereo as viewed approximately down the AC noncrystallographic 2-fold axis. The AB dimer is drawn with darker lines. Side chains for the residues involved in the internal salt bonds (Glu-43 and Lys-65 in each monomer) are shown as *connected dots*; for the four lysines on the carboxyl-terminal helix (Lys-76, -77, -80, -81 in each monomer) the side chains are shown as line segments.

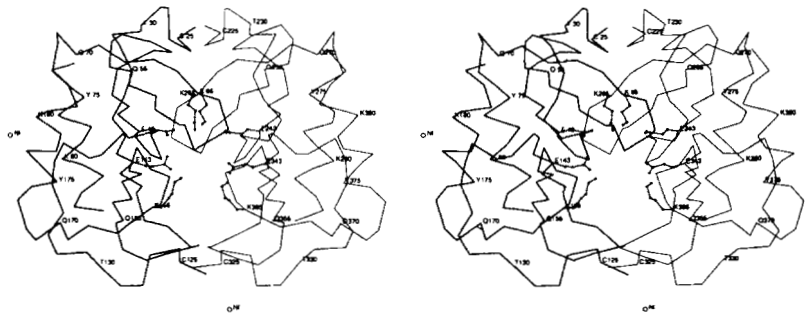

FIG. 7. **The PF4 tetramer and the nickel position.** The α-carbon backbone from the refined model of the PF4 tetramer is shown in stereo, as viewed approximately down the AD noncrystallographic 2-fold axis. The position of Tyr-75 in each monomer has been labeled to identify the monomers. *Hollow circles* mark the positions of the two nickel atoms that are shared with adjacent tetramers. Side chains are drawn as *connected dots* for the residues involved in the internal salt bonds (Glu-43 and Lys-65 in each monomer).

drogenase (Eklund *et al.*, 1976), and aspartate transcarbamylase R-chain (Krause *et al.*, 1987).

Secondary Structure—Residues Glu-1 to Leu-23 are missing due to proteolytic removal and disorder. The first 13 residues were removed with elastase prior to crystallization. The other 10 missing residues are unobserved, possibly because they include 5 acidic residues which repulse one another so strongly in the low ionic strength environment of the crystals (20 mM Tris), that they locally denature the protein. We know that the 10 residues are present because Edman sequencing of PF4 from a washed and redissolved crystal confirmed the amino-terminal sequence from Asp-14 to Gln-24.

Residues Gln-24 to Ile-34 are best described as being random coil or as forming a large, open loop. There are bends, as defined by Kabsch and Sander (1983), centered at residues 25 and 27 and one hydrogen bond from Thr-31 to Cys-67 in the β-sheet (Fig. 8). The chain is also stabilized by the two disulfide bonds Cys-25 to Cys-51 and Cys-27 to Cys-67. Residues Asn-35 to His-38 form an external loop that is stabilized by a main chain hydrogen bond (38N $\rightarrow$ 35O). It does not reverse the direction of the polypeptide chain and could be viewed as a single turn of helix.

Residues Ile-39 to Ser-46, which comprise strand I of the three-stranded β-sheet in the monomer, also form six main chain hydrogen bonds (Fig. 8) with the adjacent monomer in the extended β-sheet. Leu-42 and Val-44 contact the hydrophobic surface of the carboxyl-terminal helix. Glu-43 on the "interior side" of the β-sheet in monomer A forms an internal salt bridge with Lys-265 of monomer C in the other extended β-sheet and similarly for the related pair Glu-243/Lys-65. The respective Glu-OE1 to Lys-NZ distances are 2.77 and 3.22 Å. The comparable salt bridges between monomers B and D, namely Glu-143/Lys-365 and Glu-343/Lys-165, which have Glu-OE1 to Lys-NZ distances of 9.65 and 8.67 Å, respectively, are presumably not made in this particular crystal form due to distortion by the nickel substitution.

Residues Ala-47 to Ser-53 form a hairpin loop (Sibanda and Thornton, 1985) between strands I and II of the β-sheet. There is an atypical 14-atom turn involving a hydrogen bond from Gly-48 to Cys-51. Residues Pro-54 to Thr-59 and Arg-64 to Leu-68 form strands II and III, respectively, of the β-sheet. They are linked by residues Lys-60 to Gly-63, which form a hydrogen-bonded reverse turn. In the rat (Doi *et al.*, 1987) and human[3] genes for PF4, an intron occurs between residues 57 and 58 in strand II. There are two β-bulges (Richardson, 1981); a wide type at Ile-39/Ser-40 and a G type at Gly-63/Arg-64.

Residues Gln-70 to Leu-74 loop between strand III and a helix at the end of the molecule. There is a hydrogen bond between Gln-70 and Arg-72 which forms an inverse γ-turn (Rose *et al.*, 1985). Residues Tyr-75 to Gly-85 form an α-helix that lies diagonally across the top of the β-sheet. Since the axis of the helix follows the slope from the saddle point of the sheet rather than the rise, this packing arrangement falls into class 2 of Chou *et al.* (1985) rather than class 4. Although the former is less favored energetically in theoretical calculations, the difference is less for antiparallel β-sheets than for parallel ones.

The secondary structure that we observe for residues 24–85 of bovine PF4 differs significantly from that predicted by the Chou and Fasman algorithm (Lawler, 1981) for human PF4, which should have essentially the same overall structure as the bovine protein. We observe 18% α-helix, 29% β-sheet, 19% reverse turn, and 34% unordered coil, whereas the pre-

[3] M. Poncz, personal communication.

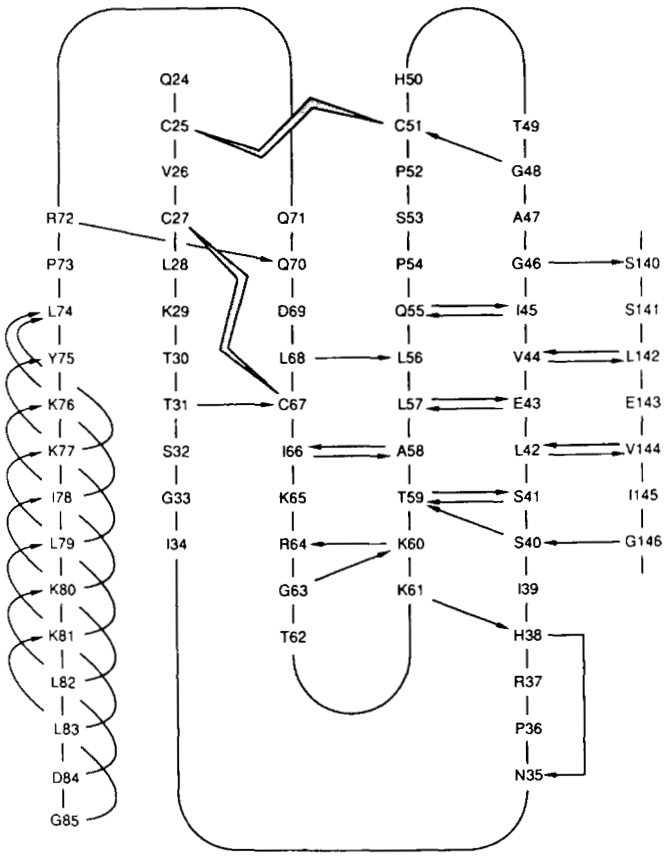

FIG. 8. **Hydrogen bonds and topology of PF4.** The four loops, three strands of β-sheet, and one α-helix found in the PF4 monomer are indicated in a diagram of the topology of the monomer. The two cystine bonds are shown as *shaded lines*. The main chain hydrogen bonds, as determined by the graphic display program QUANTA, are shown by arrows going from the donor to the acceptor. The criteria for a hydrogen bond are that the angles C=O···H, O···H–N, and H–N–C be greater than 90°, and that the distance N···O not exceed 3.3 Å for a "short" hydrogen bond and 4.0 for a "long" one (Baker and Hubbard, 1984). A hydrogen bond was included in the diagram if it was present in all four subunits and was a short bond in at least one of them. Exceptions to these criteria are the bonds S41 → T59 and D84 → K80 which were long in all the subunits, and R72 → Q70 which was short in subunits A and D but absent in subunits B and C, which instead had a long hydrogen bond to D69. Several hydrogen bonds within the helix, namely K80 → K77, K81 → I78, D84 → K80, and G85 → K81, which were short in at least one subunit, were not included because they were missing in other subunits.

dicted structure is 55% α-helix, 18% β-sheet, 26% reverse turn, and 1% unordered coil. The predicted structure for the large open loop is a strand of β-sheet and a reverse turn; for the short, external loop, another reverse turn; for strand I, helix; for strand II, helix; for strand III, β-sheet and helix; and for the γ-reverse turn, helix. The reverse turns at residues 47–50 and 61–63 are predicted correctly to within a few residues, as is the carboxyl-terminal helix. Furthermore, the prediction that the four lysines implicated in binding heparin would be clustered on one side of a helix is verified in our structure.

An exact comparison between the distribution of secondary structure in our model and that measured by circular dichroism on human PF4 (Villanueva *et al.*, 1988), namely 15% α-helix, 25% β-structure, and 60% unordered coil, is not possible because the first 10 residues are disordered in our crystals. However, taken at face value, the circular dichroism measurements imply that these 10 residues are neither α-helix nor β-sheet.

Tertiary and Quaternary Interactions—Along with the intrachain disulfide and hydrogen bonds, there are several clusters of hydrophobic residues which contribute significantly to the integrity of the monomer structure. Residues Ile-34 and Pro-36 at the end of the random coil form a cluster with residues Ile-39, Ile-66, and Leu-68 in the β-sheet and residues Leu-74 and Ile-78 in the α-helix. At the helix-sheet interface residues Leu-42, Val-44, and Leu-56 in the β-sheet are together with residues Tyr-75, Leu-79, and Leu-83 in the α-helix.

The A/B dimer is maintained by six hydrogen bonds (Fig. 8) and by the cluster of hydrophobic residues at the helix-sheet interface which extends into the adjacent monomer to include residues Leu-142, Val-144, Leu-156, Tyr-175, Leu-179, and Leu-183. Only 3 of the 12 residues in subunit B that are within 3.5 Å of a residue in subunit A are hydrophilic. The inner hydrophobic surfaces of the α-helices actually overlap the β-sheet strands from the adjacent monomer. A consequence of these interactions is that the shallow groove between the two helices, which has a floor defined by Leu-42, Val-44, Pro-54, Leu-56, and the equivalent residues in subunit B, and walls defined by residues Gln-70, Tyr-75, Leu-79, Leu-83, and the equivalent residues in subunit B, is quite hydrophobic.

Hydrophobic interactions are also evident at the interface of the A/B and C/D dimers. Residue Val-26 at the beginning of the long stretch of random coil and residues Ile-45 and Leu-57 in the β-sheet cluster with the equivalent residues in subunit C. However, the interface between the two dimers, which contains the four buried salt links discussed previously, appears to be predominantly hydrophilic. Seven of the 10 residues in subunits C and D that are within 3.5 Å of a residue in subunit A are hydrophilic.

Additional evidence for the structural significance of these interactions comes from the conservation of specific residues in the sequences of proteins that are homologous to PF4. As shown in Fig. 9, the salt link between positions 43 and 65 is conserved in the sequences of all proteins homologous to PF4 with the sole exception of the human GRO protein. In the Chinese hamster GRO protein, protein 9-E3, and protein 3-10C, the acidic and basic residues have switched positions in the sequence. In protein 3-10C, lysine is replaced by arginine at position 43. Also, in almost all the homologs, hydrophobic residues occupy the same 12 positions identified above as having important structural roles in PF4. Hydrophilic residues occur once at position 66 and 74 and four times at position 83.

Nickel Site—The structures of the four subunits in the crystallographic asymmetric unit are quite similar; the largest root mean square deviation between main chain coordinates is 0.69 Å for subunits A and D. The tetramer, however, is significantly asymmetric. Its distortion from 222 symmetry in the structure reported here is caused by the $Ni(CN)_4^{2-}$ ions, which insert between tetramers along the *b*-axis of the crystals and increase the axis by 1.45 Å. The β-bilayer is pried open along the BD edge by approximately 5 Å measured between the amino termini of the two subunits. Four residues have non-carbon atoms within 6 Å of the two nickel sites that bracket each tetramer, namely, Cys-325 and Gln-324 (N) in subunit B and Lys-181 and Lys-177 in subunit D. Lys-181, in particular, seems to make a specific contact (NZ to Ni is 2.19 Å). Although the tetramer, which occupies one asymmetric unit, is not under a crystallographic constraint to have 222 symmetry, it is unlikely that asymmetric crystal packing alone could cause the substantial distortions discussed above.

Heparin Binding Site—The positively charged amino acid

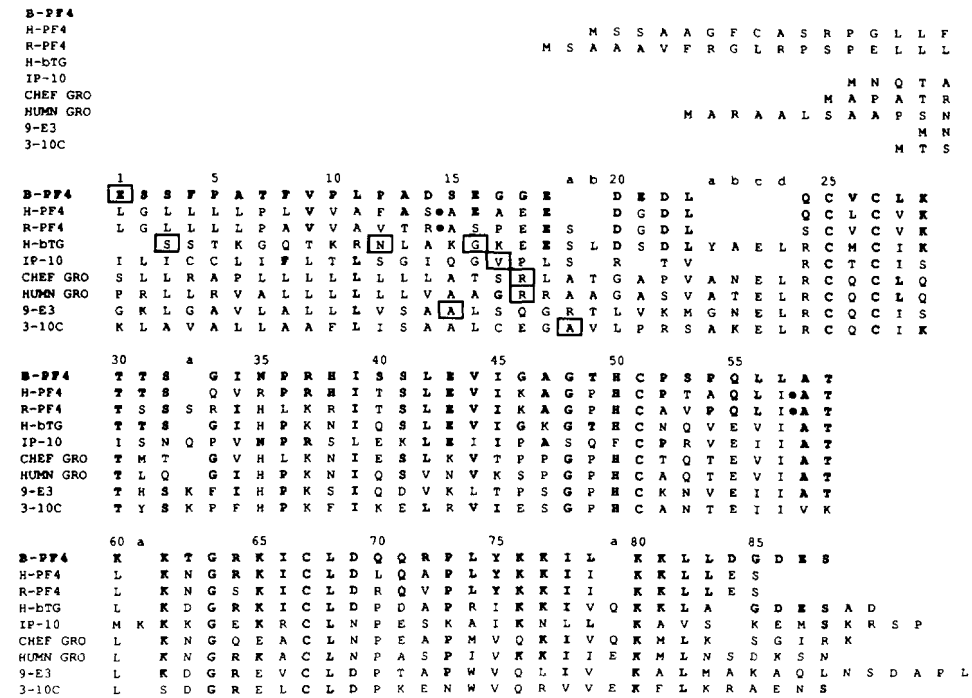

FIG. 9. **Sequences of PF4 and its homologs.** The sequences of bovine (Ciaglowski *et al.*, 1986), human (Poncz *et al.*, 1987), and rat PF4 (Doi *et al.*, 1987) are compared along with those of six homologous proteins, namely human β-thromboglobulin (*H-bTG*; Holt *et al.*, 1986), γ-interferon induced protein (*IP-10*; Luster *et al.*, 1985), Chinese hamster and human growth-related proteins (*CHEF GRO, HUMN GRO*; Anisowicz *et al.*, 1987), Rous sarcoma virus-induced protein (*9-E3*; Sugano *et al.*, 1987), and mitogen-stimulated human leukocyte protein (*3-10C*; Schmid and Weissmann, 1987). The positions are numbered according to the bovine PF4 sequence with letters for insertions. Protein 9-E3 was also reported as pCHEF-4 with leucine replacing phenylalanine at position 5 (Bedard *et al.*, 1987). Protein 3-10C was also reported as neutrophil-activating factor by Walz *et al.* (1987) and monocyte-derived neutrophil chemotactic factor by Yoshimura *et al.* (1987). The alignments with the PF4 sequence are taken from the original papers; residues identical with those in PF4 are in **boldface**. The known or putative amino-terminal residue of the mature protein is *boxed* for each sequence. For human β-TG, the amino-terminal serine of platelet basic protein (Holt *et al.*, 1986), the amino-terminal asparagine of low affinity platelet factor 4 (Rucinski *et al.*, 1979) or connective tissue-activating protein III (Castor *et al.*, 1983) and the amino-terminal glycine of β-TG (Begg *et al.*, 1978) are indicated. *Dots* indicate exon-intron boundaries in the rat (Doi *et al.*, 1987) and human[3] PF4 genes.

side chains, especially the cluster of four lysines (Lys-76, -77, -80, -81) near the carboxyl-terminal end, are of paramount importance in binding heparin (Handin and Cohen, 1976). The refined positions of the four lysine side chains are shown in Fig. 4 and 6. Lysine side chains, which are usually on the surface and highly mobile, are often disordered in crystal structures. In Fig. 4, some electron density, albeit discontinuous, is seen for all four lysine side chains. The side chain of Lys-81 is the best ordered of the four. The lysines are bunched on the side of the helix that is opposite to the helix of the neighboring monomer (Fig. 6). Lawler (1981) showed that the spacing of the four lysines in the PF4 sequence would put them together on one side of the helix that he had predicted for the carboxyl-terminal end of PF4. β-Thromboglobulin, a proteolyzed derivative of platelet basic protein, has a lower affinity for heparin than does PF4. Lawler (1981) pointed out that the extra residue (Gln-79a in Fig. 9) between the pairs of lysine residues in β-TG would create a staggered rather than in-line arrangement of the lysines. Our model of PF4 predicts that one of the lysines in β-TG, either 76 or 81, is buried between the carboxyl-terminal helix and the β-sheet.

To our knowledge, no other three-dimensional structure of a heparin-binding protein is known. In a similar fashion to Lawler's analysis of the PF4 sequence, Villaneuva (1984) has proposed a model of the heparin binding site in AT-III based on prediction of secondary structure and chemical modification experiments. A helix containing lysines 282, 286, and 299 would have the three positive charges on the same side and optimally arranged to interact with three critical sulfates on the octasaccharide binding unit in heparin that is preferred by AT-III.

In the absence of a structure of the heparin-PF4 complex, we can only speculate as to how the complex might be formed. The negatively charged heparin has been shown to wrap around the outside of the PF4 tetramer (Ibel *et al.*, 1986) and to interact specifically with lysine residues. Handin and Cohen (1976) showed that guanidination, which changes the structure but not the charge of the lysines, greatly reduced the binding of heparin while modifications to the arginine residues had no effect. A preliminary analysis suggests two possible structures for the heparin complex. The polysaccharide chain could pass along the shallow hydrophobic groove between the two helices of each dimer or it could cross-over the helices more or less at right angles. The latter route would follow a belt of positively charged residues around the PF4 tetramer. However, heparin binding to PF4, which is not a very cationic protein (pI = 7.6; Handin and Cohen, 1976), need not be entirely electrostatic, as shown by related experiments on antithrombin. Although heparin binds specifically to lysine residues on antithrombin (Rosenberg and Damus, 1973), the overall interaction is nonelectrostatic (Heuck *et al.*, 1985) and also involves specific tryptophan residues in anti-

thrombin (Einarsson and Andersson, 1977; Villanueva *et al.*, 1980).

Acknowledgments—We are indebted to Wayne Hendrickson, B. C. Wang, George Reeke, and Paul Bethge for sending us computer programs used in this work.

REFERENCES

Anisowicz, A., Bardwell, L., and Sager, R. (1987) *Proc. Natl. Acad. Sci. U. S. A.* **84,** 7188–7192

Baker, E. N., and Hubbard, R. E. (1984) *Prog. Biophys. Mol. Biol.* **44,** 97–179

Barber, A. J., Käser-Glanzmann, R., Jakabova, M., and Luscher, E. F. (1972) *Biochim. Biophys. Acta* **286,** 312–329

Bedard, P.-A., Alcorta. D., Simmons, D. L., Luk, K.-C., and Erikson, R. L. (1987) *Proc. Natl. Acad. Sci. U. S. A.* **84,** 6715–6719

Begg, G. S., Pepper, D. S., Chesterman, C. N., and Morgan, F. J. (1978) *Biochemistry* **17,** 1739–1744

Bjorkman, P. J., Saper, M. A., Samraoui, B., Bennett, W. S., Strominger, J. L., and Wiley, D. C. (1987) *Nature* **329,** 506–512

Blake, C. C. F. Geisow, M. J., Swan, I. D. A., Rerat, C., and Rerat, B. (1974) *J. Mol. Biol.* **88,** 1–12

Bock, P. E., Luscombe, M., Marshall, S. E., Pepper, D. S., and Holbrook, J. J. (1980) *Biochem. J.* **191,** 769–776

Castellot, J. J., Jr., Favreau, L. V., Karnovsky, M. J., and Rosenberg, R. D. (1982) *J. Biol. Chem.* **257,** 11256–11260

Castor, C. W., Miller, J. W., and Walz, D. A. (1983) *Proc. Natl. Acad. Sci. U. S. A.* **80,** 765–769

Chou, K-C., Nemethy, G., Rumsey, S., Tuttle, R. W., and Sheraga, H. A. (1985) *J. Mol. Biol.* **186,** 591–609

Ciaglowski, R. E., Snow, J., and Walz, D. A. (1981) *Ann. N. Y. Acad. Sci.* **370,** 668–679

Ciaglowski, R. E., Snow, J. W., and Walz, D. A. (1986) *Arch. Biochem. Biophys.* **250,** 249–256

Cowan, S. W., Bakshi, E. N., Machin, K. J., and Isaacs, N. W. (1986) *Biochem. J.* **234,** 485–488

Creighton, T. E. (1984) *Proteins*, p. 234, W. H. Freeman and Co., New York

Denton, J., Lane, D. A., Thunberg, L., Slater, A. M., and Lindhal, U. (1983) *Biochem. J.* **209,** 455–460

Deuel, T. F., Keim, P. S., Farmer, M., and Heinrikson, R. L. (1977) *Proc. Natl Acad. Sci. U. S. A.* **74,** 2256–2258

Deuel, T. F., Sonior, R. M., Chang, D., Griffin, G. L., Heinrikson, R. L., and Kaiser, E. T. (1981) *Proc. Natl. Acad. Sci. U. S. A.* **78,** 4584–4587

Doi. T., Greenberg, S. M., and Rosenberg, R. D. (1987) *Mol. Cell. Biol.* **7,** 898–904

Einarsson, R., and Anderson, L. O. (1977) *Biochim. Biophys. Acta* **490,** 104–111

Eklund, H., Nordstrom, B., Zippezauer, E., Soderlund, G., Ohlsson, I., Boiwe, T., Soderberg, B.-O., Tapia, O., Banden, C.-I., and Akeson, A. (1976) *J. Mol. Biol.* **102,** 27–59

Handin, R. I., and Cohen, H. J. (1976) *J. Biol. Chem.* **251,** 4273–4282

Hendrickson, W. A., and Konnert, J. H. (1980) in *Biomolecular Structure, Function, Conformation, and Evolution* (Srinivasan, R., ed) pp. 43–57, Pergamon Press. Oxford

Hendrickson, W. A. (1985) *Methods Enzymol.* **115,** 252–270

Hermodson, M. A., Schmer, G., and Kurachi, K. (1977) *J. Biol. Chem.* **252,** 6267–6279

Heuck, C. C., Schiele, U., Horn, D., Fronda, D., and Ritz, E. (1985) *J. Biol. Chem.* **260,** 4598–4603

Holt, J. C., Harris, M. E., Holt, A. M., Lange, E., Henschen, A., and Niewiarowski, S. (1986) *Biochemistry* **25,** 1988–1996

Ibel, K., Poland, G. A., Baldwin, J. P., Pepper, D. S., Luscombe, M., and Holbrook, J. J. (1986) *Biochim. Biophys. Acta* **870,** 58–63

Kabsch, W., and Sander, C. (1983) *Biopolymers* **22,** 2577–2637

Kaser-Glanzmann, R., Jakabova, M., and Luscher, E. F. (1972) *Experimentia* **28,** 1221–1223

Katz, I. R., Thorbecke, G. J., Bell, M. K., Yin, J.-Z., Clarke, D., and Zucker, M. B. (1986) *Proc. Natl. Acad. Sci. U. S. A.* **83,** 3491–3495

Krause, K. L., Volz, K. W., and Lipscomb, W. N. (1987) *J. Mol. Biol.* **193,** 527–553

Kreiger, M., Chambers, J. L., Christoph, G. G., Stroud, R. M., and Trus, B. L. (1974) *Acta Crystallogr. Sect. A Found. Crystallogr.* **30,** 740–748

Kurachi, K. (1978) *J. Biol. Chem.* **253,** 8301–8302

Laurent, T. C., Tengblad, A., Thunberg, L., Höök, M., and Lindahl, U. (1978) *Biochem. J.* **175,** 691–701

Lawler, J. W. (1981) *Thromb. Res.* **21,** 121–127

Loscalzo, J., Melnick, B., and Handin, R. I. (1985) *Arch. Biochem. Biophys.* **240,** 446–455

Luscombe, M., and Holbrook, J. J. (1983) in *Glycoconjugates* (Chester, A. M., Heinegard, D., Lundblad, A., and Svensson, S., eds) pp. 818–819, Secretariat, Lund

Luster, A. D., Unkeless, J. C., and Ravetch, J. V. (1985) *Nature* **315,** 672–676

Machin, K. J., and Isaacs, N. W. (1984) *J. Mol. Biol.* **172,** 221–222

Machovich, R. (1984) in *The Thrombin* (Machovich, R., ed) Vol. I, p. 1, CRC Press, Boca Raton, FL

Morgan, F. J., Begg, F. S., and Chesterman, C. M. (1977) *Thromb. Haemostasis* **38,** 231–235

North, A. C. T., Phillips, D. C., and Matthews, F. S. (1968) *Acta Crystallogr. Sect. A Found. Crystallogr.* **24,** 351–359

Poncz, M., Surrey, S., LaRocco, P., Weiss, M. J., Rappaport, E. F., Conway, T. M., and Schwartz, E. (1987) *Blood* **69,** 219–223

Reeke, G. N. (1984) *J. Appl. Crystallogr.* **17,** 125

Reeke, G. N., Jr., Becker, J. W., and Edelman, G. M. (1975) *J. Biol. Chem.* **250,** 1525–1545

Richardson, J. (1981) *Adv. Protein Chem.* **34,** 167–339

Rose, G., Gierasch, L. M., and Smith, J. A. (1985) *Adv. Protein Chem.* **37,** 1–109

Rosenberg, R. D., and Damus, P. S. (1973) *J. Biol. Chem.* **248,** 6490–6505

Rucinski, B., Niewiarowski, S., James, P., Walz, D. A., and Budzynski, A. Z. (1979) *Blood* **53,** 47–62

Schmid, J., and Weissmann, C. (1987) *J. Immunol.* **139,** 250–256

Senior, R. M., Griffin, G. L., Huang, J. S., Walz, D. A., and Deuel, T. D. (1983) *J. Cell Biol.* **96,** 382–385

Sibanda, B. L., and Thornton, J. M. (1985) *Nature* **316,** 170–174

St. Charles, R., Ciaglowski, R. E., Walz, D., and Edwards, B. F. P. (1984) *J. Mol. Biol.* **176,** 421–423

Stern, D., Nawroth, P., Marcum, J., Handley, D., Kisiel, W., Rosenberg, R. D., and Stern, K. (1985) *J. Clin. Invest.* **75,** 272–279

Sugano, S., Stoeckle, M. Y., and Hanafusa, H. (1987) *Cell* **49,** 321–328

Taylor, S., and Folkman, J. (1982) *Nature* **297,** 307–312

Twardzik, D. R., and Todaro, G. J. (1987) U. S. Patent 4,645,828

Villanueva, G. B. (1984) *J. Biol. Chem.* **259,** 2531–2536

Villanueva, G. B., Perret, V., and Danishefsky, I. (1980) *Arch. Biochem. Biophys.* **203,** 453–457

Villanueva, G. B., Allen, N., and Walz, D. (1988) *Arch. Biochem. Biophys.* **261,** 170–174

Walz, D. A., Wu, V. Y., de Lamo, R., Dene, H., and McCoy, C. E. (1977) *Thromb. Res.* **11,** 893–898

Walz, A., Peveri, P., Aschauer, H., and Baggiolini, M. (1987) *Biochem. Biophys. Res. Commun.* **149,** 755–761

Wang, B.-C. (1985) *Methods Enzymol.* **115,** 90–111

Yoshimura, T., Matshshima, K., Tanaka, S., Robinson, E. A., Appella, E., Oppenheim, J. J., and Leonard, E. J. (1987) *Proc. Natl. Acad. Sci. U. S. A.* **84,** 9233–9237